IEEE Access
Multidisciplinary | Rapid Review | Open Access Journal

Received May 19, 2020, accepted June 29, 2020, date of publication July 2, 2020, date of current version July 15, 2020.

Digital Object Identifier 10.1109/ACCESS.2020.3006483

Experimental Analysis of Cooling Fan Noise by Wavelet-Based Beamforming and Proper Orthogonal Decomposition

SICONG LIANG[1], WANGQIAO CHEN[1], RHEA P. LIEM[2], AND XUN HUANG[1,2], (Member, IEEE)

[1]State Key Laboratory of Turbulence and Complex Systems, Aeronautics and Astronautics, College of Engineering, Peking University, Beijing 100871, China
[2]Department of Mechanical and Aerospace Engineering, The Hong Kong University of Science and Technology, Hong Kong

Corresponding author: Wangqiao Chen (chenwangqiao@pku.edu.cn)

The work of Xun Huang was supported in part by the National Science Foundation of China under Grant 91852201, and in part by the Research Grants Council of the Hong Kong Special Administrative Region under Grant 16205317.

ABSTRACT We use the proper orthogonal decomposition (POD) method to decompose acoustic imaging from wavelet-based beamforming results into their corresponding modes, and demonstrate the method to analyze the noise characteristics of small-dimensional components, where research literature is still scarce. In particular, we consider the noise from a central processing unit (CPU) cooling fan, though the developed method could find realistic applications in a wider scheme of electronic industry. In addition to developing the new analysis method, we also endeavor to prepare a realistic experimental setup with a CPU cooling fan in an anechoic room. The results show that the combination of POD and wavelet-based beamforming methods is suitable for CPU cooling fan acoustic imaging, which can enhance the analysis ability of acoustic imaging test. The results offered in this work are helpful in cooling fan design and evaluation, which would open doors to a wide range of industrial applications.

INDEX TERMS Acoustic imaging, proper orthogonal decomposition, fan noise, wavelet.

I. INTRODUCTION

An experimental study is conducted in this work for cooling fan noise by combining advanced analysis methods of proper orthogonal decomposition (POD) and wavelet-based beamforming. The noise reduction issue of cooling fan, which have been heavily used in central processing unit (CPU)/graphics processing unit (GPU), has recently become a popular topic in industry and consumer electronics and calls for a deep understanding of its acoustic physics [1]–[4]. Further insight into the underlying mechanisms would enable new technological directions such as in the further development of serrated fan and supersonic fan designs. To date, the related studies have been primarily focused on applications from huge-dimensional wind turbines [5] to large-dimensional aeroengine fans [6]–[13], whereas an experimental studys of small to tiny-dimensional CPU/GPU cooling fans are still rare. To address this issue, here we endeavor to develop and demonstrate the associated experimental and analysis methods, which constitutes the main contribution of this article.

The associate editor coordinating the review of this manuscript and approving it for publication was Ananya Sen Gupta.

In this work, we incorporate wavelet and POD analysis methods into beamforming method [14]–[19]. The latter has been commonly used in acoustic imaging with a microphone array to identify dominant noise sources [5]–[8], [20]. Wavelet-based beamforming, as one of the most recent extensions of beamforming [21], [22], works in the time-frequency domain and would enable experimental studies of unsteady noise sources [23]. It is well known that the rotating source will generate tonal noise at a certain "blade passing frequency" (BPF) and broadband noise elsewhere [24]–[26]. The former can be largely suppressed by reducing aerodynamic loading and flow separation [27]. As a result, instead of tonal noise, turbulence noise of distinctive modes at various other frequencies becomes increasingly more important [28], [29], which calls for a new analysis method.

In fluid and acoustic physics, POD has been commonly used to decompose physical fields into several constituting modes, which can help elucidate short-term, transient fluid dynamics, such as the coherent structures and instability of turbulence [30]–[38]. Considering the similarity between acoustic imaging and flow field, here we combine POD and beamforming methods together to decompose

acoustic imaging results into their corresponding basic POD modes. More interestingly, it seems that POD mode results can be correlated to circumferential modes and radial modes in the spatial domain, which suggests that POD can serve as fan noise mode detections in a physical sense [30], [31], [39]–[43].

In this article, we decompose the modes of acoustic images from a cooling fan noise by combining the POD method and the wavelet-based beamforming method. To the best of our knowledge, such a combination is still absent in experimental studies for industry electronic applications. The remaining part of this paper is organized as follows. First, the mathematical framework of the wavelet-based beamforming and POD method is summarized in Sec. II. Next, an experimental demonstration is discussed in Sec. III, which clearly shows the strength of the proposed new method that combines both POD and wavelet-based beamforming. Finally, we present the concluding remarks in Sec. IV.

II. METHODS

A. WAVELET-BASED BEAMFORMING

For the convenience of readers, here we provide the main mathematical framework of the wavelet-based beamforming method and the associated basic concepts and physical meanings. For more details, interested readers can refer to [22], [23]. Readers who are just interested in experimental demonstrations can directly jump to the next section.

We first assume the location of microphones and imaging points at $\vec{x}$ and $\vec{r}$, and consider the sound pressure p of angular frequency ω. By using wavelet transform, sound pressure can be represented in the time-frequency domain as follows:

$$P_\psi(\vec{r},\vec{x},t,s)=\frac{1}{s}\int_{-\infty}^{\infty}\psi^*\left(\frac{\tau-t}{s}\right)\cdot p(\vec{x},\tau)d\tau, \tag{1}$$

where $(\cdot)^*$ denotes a complex conjugate and s is the scale parameter of the Morse wavelet ψ. If Doppler effect α due to the movement of sources is taken into consideration, from the relationship between the emission time t_e and time t, the array measurements form the following vector:

$$Y(\vec{r},\omega,t_e)=\left[P_\psi\left(\vec{r},\vec{x}_1,t_1,\frac{s}{\alpha_1}\right)\ldots P_\psi\left(\vec{r},\vec{x}_n,t_n,\frac{s}{\alpha_n}\right)\right]. \tag{2}$$

Here $t_i = t_e + |\vec{r}-\vec{x}_i|/c_0$, $(\cdot)_i$ denotes the ith sensor of the array and c_0 is the speed of sound. Similar to the conventional beamforming method, the associated array cross spectral matrix would be

$$CSM(\vec{r},\omega,t_e)=Y(\vec{r},\omega,t_e)\cdot Y^*(\vec{r},\omega,t_e). \tag{3}$$

Following [22], [23], the free space Green's function can be written as,

$$G(\vec{r},\vec{x})=\frac{\alpha^2\beta}{4\pi|\vec{r}-\vec{x}|}, \tag{4}$$

where β collectively represents the acceleration effect of the movement of source and the near-field effect. To define the weight vector, we set $\vec{G}=[G_1\ldots G_n]$. The wavelet-based beamforming weight vector can be written as

$$\vec{w}(\vec{r},t_e)=\frac{\vec{G}(\vec{r},t_e)}{||\vec{G}(\vec{r},t_e)||}, \tag{5}$$

where $||\cdot||$ represents the $L2$-norm. By following the classical analytical form of conventional beamforming approaches, we propose the wavelet-based beamforming as

$$b(\vec{r},\omega,t_e)=\vec{w}^*(\vec{r},t_e)CSM(\vec{r},\omega,t_e)\vec{w}(\vec{r},t_e). \tag{6}$$

The wavelet-based beamforming approach shown in (6) is suitable for imaging in time-frequency analysis.

B. POD METHOD

The POD method used in this work is the so-called 'snapshot POD'. Here the number of snapshots k is equal to the number of samples of an array. By further assuming the sampling number of an array system, and the number of imaging points m, we can generate a matrix

$$B=\begin{bmatrix} b(\vec{r}_1,\omega,t_1) & \ldots & b(\vec{r}_1,\omega,t_j) & \ldots & b(\vec{r}_1,\omega,t_k)\\ \vdots & \ddots & \vdots & \ddots & \vdots\\ b(\vec{r}_j,\omega,t_1) & \ldots & b(\vec{r}_j,\omega,t_j) & \ldots & b(\vec{r}_j,\omega,t_k)\\ \vdots & \ddots & \vdots & \ddots & \vdots\\ b(\vec{r}_m,\omega,t_1) & \ldots & b(\vec{r}_m,\omega,t_j) & \ldots & b(\vec{r}_m,\omega,t_k)\end{bmatrix}, \tag{7}$$

where $\vec{r}_i$ and t_j denote the ith imaging point and the jth sampling time. The autocovariance matrix is defined as

$$R=B^*B. \tag{8}$$

Let the ordered eigenvalues λ of R is $\lambda_1\geq\lambda_i\geq\lambda_k\geq 0$, and the associated eigenvectors $\vec{\varphi}$ have the relationship

$$R\vec{\varphi}_i=\lambda_i\vec{\varphi}_i. \tag{9}$$

Here $(\cdot)_i$ denotes the ith POD mode. Next, the POD mode $\vec{\phi}_i$ can be given by

$$\vec{\phi}_i=\frac{1}{\sqrt{\lambda_i}}B\vec{\varphi}_i, \tag{10}$$

which can be easily calculated in MATLAB by using the svd function.

Fig. 1 shows the relationship between the acoustic imaging results and POD method. In particular, the results indicate that the wavelet-based beamforming can provide the unprecedented analysis capability in space, time, and frequency simultaneously. Furthermore, Fig. 1 shows the POD results from the wavelet-based beamforming results at 5 kHz. It is worthwhile to mention that the incorporation of POD into the wavelet-based beamforming is straightforward to implement. The corresponding steps are summarized as follows:

1) Calculate the wavelet transform for each sensor.
2) Generate the array outputs $Y(\vec{r},\omega,t_e)$.
3) Calculate the weight vector for every imaging point at each imaging time.
4) Generate the cross spectral matrix for every imaging point at each imaging time.

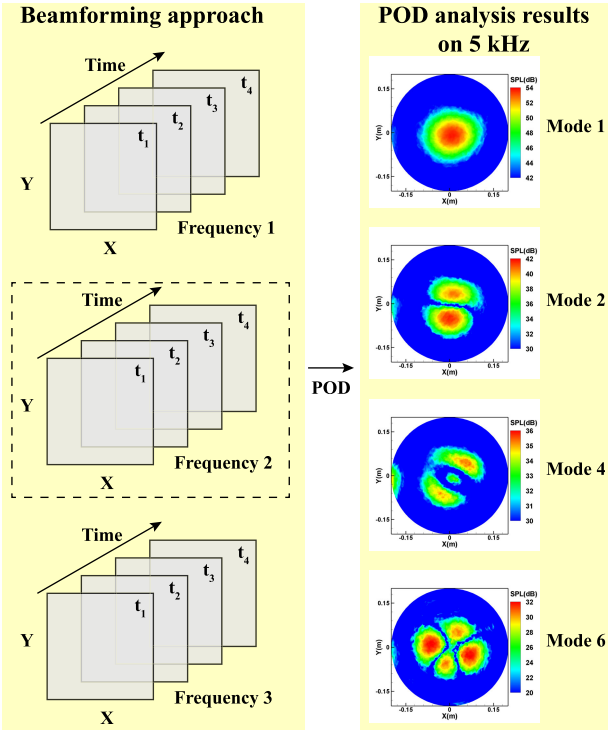

FIGURE 1. Sketch of the combination of the wavelet-based beamforming method and POD method together.

5) Calculate the wavelet-based beamforming results by following (6).
6) Conduct POD analysis at a frequency of interest and produce the corresponding POD modes.

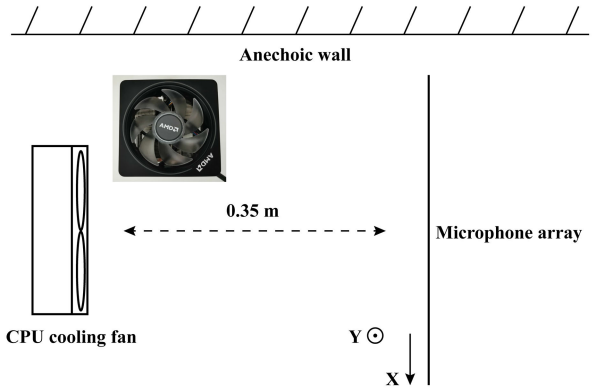

FIGURE 2. Experimental setup in the half-anechoic room.

III. EXPERIMENTAL DEMONSTRATION

In this paper, we focus on applying the proposed method to experimentally analyze the noise images from a practical CPU cooling fan, which shall serve as a good demonstration. The experiment is carried out in a half-anechoic room. Fig. 2 shows the top view of the experimental setup. The CPU cooling fan (AMD Wraith Prism with the diameter $D = 90$ mm) is placed on the left hand side of the setup, as shown in Fig. 2, with the rotating speed of 2650 rpm and 3960 rpm, respectively. The distance between the microphone array and the CPU cooling fan is 0.35 m.

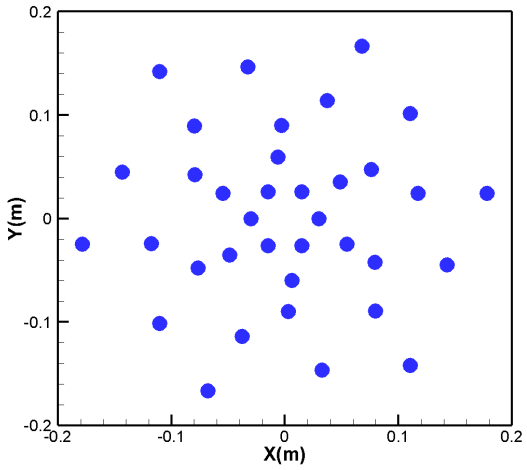

FIGURE 3. The layout of the microphone array used in this work.

A microphone array of 36 Brüel & Kjær type 4957 high-precision sensors (with a linear response between 50 Hz and 10 kHz) is adopted. The sensors are validated by the pistonphone at 98 dB/1 dB. The layout of the microphones is shown in Fig. 3. The simultaneous sampling rate is set to 50 kHz for a total sampling period of 4 s. The data acquisition is performed by using a NI PXI-1071 chassis with three 24-bit PXI-4496 cards.

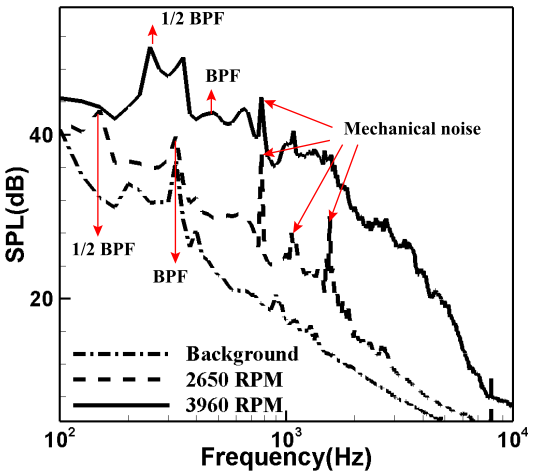

FIGURE 4. The averaged SPL results from the microphone array at three various setups.

Before showing acoustic images, Fig. 4 first shows the averaged SPL results from the microphone array, where the dashed line is the SPL results at 2650 rpm, solid line at 3960 rpm and the dash-dot line is the background noise. In addition to BPF noise and its harmonics, the SPL results consist of half-BPF tones (the first subharmonic) and broadband noises. The former could be caused by the unsteady wake-rotor interaction. Some other high-frequency tones are directly related to mechanical vibrations. Moreover, physically, the broadband noise at high frequency ranges is mainly from flow turbulence.

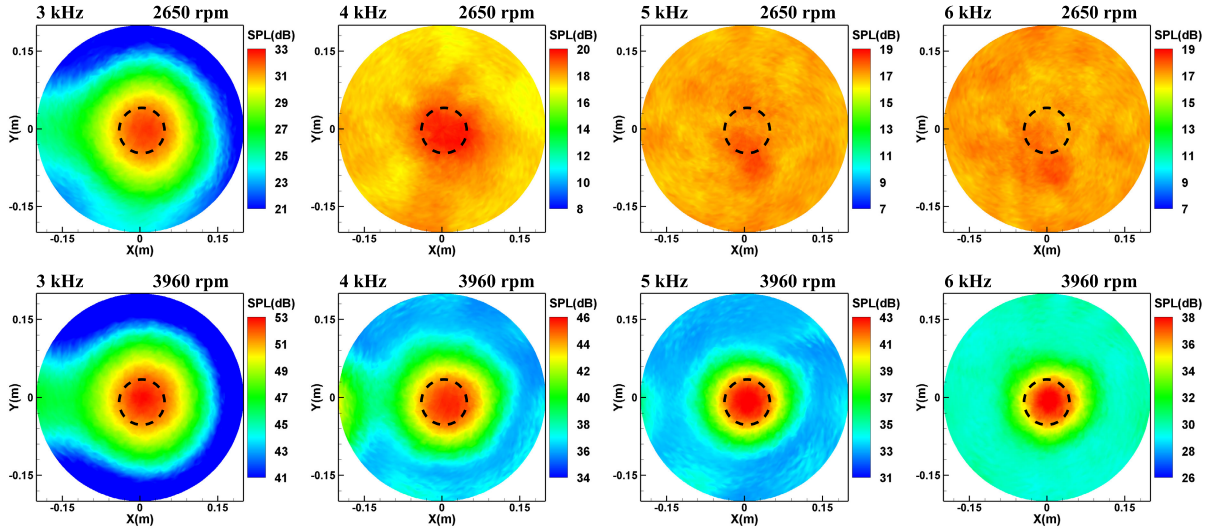

FIGURE 5. Time averaged wavelet-based beamforming results with different rotating speed and different frequencies.

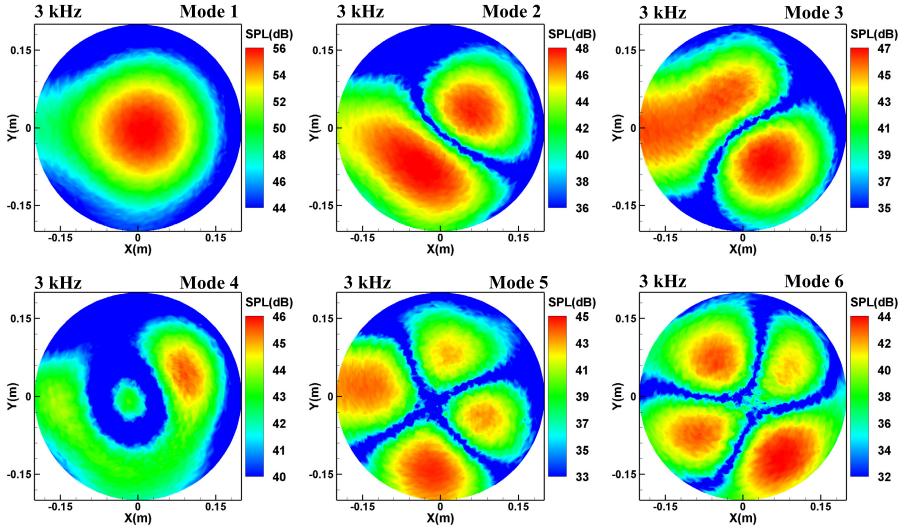

FIGURE 6. The POD results from the wavelet-based beamforming at 3 kHz with 2650 rpm, where mode 1 corresponds to the results with $(m, n) = (0, 0)$, mode 2 and mode 3 to $(m, n) = (1, 0)$, mode 4 to $(m, n) = (0, 1)$, mode 5 and mode 6 to $(m, n) = (2, 0)$.

Next, when applying the wavelet-based beamforming method, the imaging resolution limit is directly proportional to the array aperture and the frequency of target sound components. In practice, the acoustic imaging results would be incorrect when the array achieves its diffraction limit, which is especially stringent for high-frequency noise from a small cooling fan. Moreover, Fig. 4 shows that the noise level at 2650 rpm is close to the background noise level across most frequencies, whereas the noise level at 3960 rpm is much greater by around 20 dB. Hence, the following analysis is mostly focused on the setup with 3960 rpm.

Fig. 5 shows the time-averaged wavelet-based beamforming results at two different rotating speeds and a couple of representative frequencies, from 3 kHz to 6 kHz. In the figures the dashed circle denotes the size and the location of the cooling fan. Here the frequencies are deliberately chosen to be much greater than the BPF because the study is focused on high-frequency turbulence noise physics. The dynamic range of the results is set to 12 dB. At the lower rpm setup, Fig. 4 already shows that the associated noise level approaches the background noise level (smaller than 3 dB beyond 3 kHz). Hence, the imaging results at the higher rpm (3960 rpm, the bottom row of Fig. 5) is less susceptible to background noise interference.

Next, by observing the results in Fig. 5, one may immediately argue the seemingly limited information that can be obtained by such a complicated testing system. It is not surprising that the noise source is located at the fan, and the only useful knowledge from the wavelet-based beamforming will be the relative sound pressure levels of noise sources

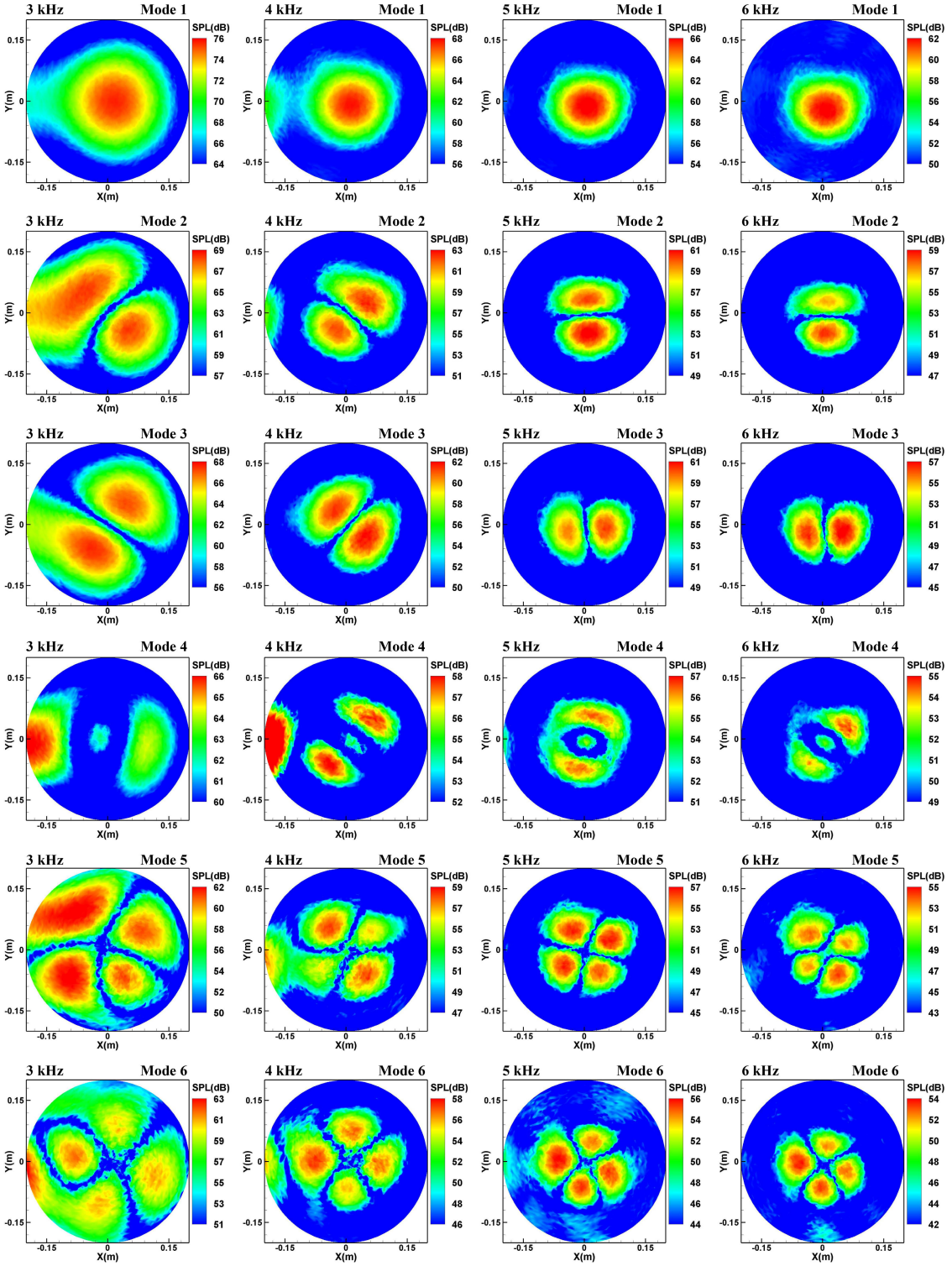

FIGURE 7. The POD results from the wavelet-based beamforming at the whole frequency range with 3960 rpm, where mode 1 corresponds to the results with $(m, n) = (0, 0)$, mode 2 and mode 3 to $(m, n) = (1, 0)$, mode 4 to $(m, n) = (0, 1)$, mode 5 and mode 6 to $(m, n) = (2, 0)$.

from different fan designs. Nevertheless, we must emphasize that such a seemingly simple image would be very helpful in cooling fan design and evaluation. Moreover, we found that more insightful knowledge can be further distilled by incorporating the POD approach into the wavelet beamforming results.

As an example, Fig. 6 shows the results of various POD modes from the beamforming image at 3 kHz and 2650 rpm

(i.e., the top left panel in Fig. 5). It can be seen that the POD method successfully decomposes the beamforming results into a couple of POD modes, which are actually closely correlated to the circumferential and radial modes that are already well-known in turbomachinery mechanics.

By following the common practice, here we assume the circumferential mode number is m and the radial mode number is n, where mode 1 corresponds to the results with $(m, n) = (0, 0)$, mode 2 and mode 3 to $(m, n) = (1, 0)$, mode 4 to $(m, n) = (0, 1)$, mode 5 and mode 6 to $(m, n) = (2, 0)$. Moreover, Fig. 7 shows the POD results for the much louder setup (at 3960 rpm) at the whole frequency range.

From Fig. 6 and Fig. 7, it can be seen that the proposed method could help to crack down the seemingly simple acoustic images to further provide quantitative information at various POD modes, which shall be closely correlated to the existing circumferential modes and radial modes. More specifically, currently, the dominant one is mode 1, which is much greater than other modes by more than 5 dB from 3 kHz to 5 kHz and 3 dB at 6 kHz. Fig. 6 and Fig. 7 show that mode 2 is greater than mode 3 by around 1 dB or 2 dB, which is smaller than the difference value between the mode 1 and mode 2. An inherent connection between these two POD modes and the physical dipole source could be established. In a similar way, higher POD modes could find their corresponding more collective physical sources (quadrupole, etc.). To this end, it is clear that our signal processing approach is able to offer distinctive physical insights that are impossible to achieve with other classical methods. Moreover, by using our approach, fan designs can be examined and evaluated quantitively at each POD mode, which could facilitate low-noise designs.

IV. CONCLUSION

In this paper, a new signal processing method has been proposed for the experimental study and analysis of cooling fan noise problems. The key achievement of this work is the experimental demonstration of the proposed testing method. The essential idea is the incorporation of the POD method into the wavelet-based beamforming. The current work is solely focused on the small-scale cooling fan setup, which shall find applications in industry and consumer electronics. In addition, the proposed method should be directly applicable to other large-scale aeroengine and turbine systems in aerospace industry.

In this work, we adopt the POD method directly into the wavelet-based beamforming. The latter imposes certain challenges in its understanding and the corresponding code implementation. Moreover, the experimental results (in particular, Fig. 6) clearly demonstrate the powerful capability of the wavelet-based beamforming method in terms of time-frequency analysis performance in practical applications.

The most important observations are summarized here. The former wavelet-based beamforming method is effective and generic, but is hard to analyze the CPU cooling fan noise with a small diameter (limited by the resolution). In contrast, the new method that combines the wavelet-based beamforming and POD method together can decompose source modes in a straightforward manner and produce acoustic images in the basic modes. To the best of our knowledge, we are the first to report this method and we believe it would see wide applications in industrial testing. Overall, the concept behind the proposed method is very straightforward and it should be easy to follow and implement by interested readers. We believe that this work should extend the current array beamforming capability and help the design and evaluation of low-noise propeller systems for robotics and aerospace applications.

REFERENCES

[1] B. Luo, W. Chu, and H. Zhang, "Tip leakage flow and aeroacoustics analysis of a low-speed axial fan," *Aerosp. Sci. Technol.*, vol. 98, Mar. 2020, Art. no. 105700.
[2] M. Kaltenbacher, A. Hüppe, A. Reppenhagen, F. Zenger, and S. Becker, "Computational aeroacoustics for rotating systems with application to an axial fan," *AIAA J.*, vol. 55, no. 11, pp. 3831–3838, Nov. 2017.
[3] A. Rynell, G. Efraimsson, M. Chevalier, and M. Abom, "Acoustic characteristics of a heavy duty vehicle cooling module," *Appl. Acoust.*, vol. 111, pp. 67–76, Oct. 2016.
[4] A. Rynell, M. Chevalier, M. Åbom, and G. Efraimsson, "Acoustic characteristics of a heavy duty vehicle cooling module," *App. Acoust.*, vol. 140, pp. 110–121, May 2018.
[5] S. Oerlemans, M. Fisher, T. Maeder, and K. Kögler, "Reduction of wind turbine noise using optimized airfoils and trailing-edge serrations," *AIAA J.*, vol. 47, no. 6, pp. 1470–1481, Jun. 2009.
[6] F. Krömer, J. Müller, and S. Becker, "Investigation of aeroacoustic properties of low-pressure axial fans with different blade stacking," *AIAA J.*, vol. 56, no. 4, pp. 1507–1518, Apr. 2018.
[7] R. Dougherty and B. Walker, "Virtual rotating microphone imaging of broadband fan noise," in *Proc. 15th AIAA/CEAS Aeroacoustics Conf. (30th AIAA Aeroacoustics Conf.)*, May 2009, p. 3121.
[8] B. Zajamsek, C. J. Doolan, D. J. Moreau, J. Fischer, and Z. Prime, "Experimental investigation of trailing edge noise from stationary and rotating airfoils," *J. Acoust. Soc. Amer.*, vol. 141, no. 5, pp. 3291–3301, May 2017.
[9] S. Moreau and M. Sanjose, "Sub-harmonic broadband humps and tip noise in low-speed ring fans," *J. Acoust. Soc. Amer.*, vol. 139, no. 1, pp. 118–127, Jan. 2016.
[10] Y.-H. Heo, J.-G. Ih, and H. Bodén, "Acoustic source identification of an axial fan in a duct considering the rotation effect," *J. Acoust. Soc. Amer.*, vol. 140, no. 1, pp. 145–156, Jul. 2016.
[11] P. Sijtsma, S. Oerlemans, and H. Holthusen, "Location of rotating sources by phased array measurements," in *Proc. 7th AIAA/CEAS Aeroacoustics Conf. Exhibit*, May 2001, pp. 2001–2167.
[12] P. Sijtsma, "Using phased array beamforming to locate broadband noise sources inside a turbofan engine," Nat. Aerosp. Lab. NLR, Amsterdam, The Netherlands, Tech. Rep. NLR-TP-2009- 689, 2006.
[13] Y. Yang, Y. Liu, H. Hu, X. Liu, Y. Wang, E. J. G. Arcondoulis, and Z. Li, "Experimental study on noise reduction of a wavy multi-copter rotor," *Appl. Acoust.*, vol. 165, pp. 11716–11726, Mar. 2020.
[14] B. D. Van Veen and K. M. Buckley, "Beamforming: A versatile approach to spatial filtering," *IEEE ASSP Mag.*, vol. 5, no. 2, pp. 4–24, Apr. 1988.
[15] J. Li and X. Zhang, "Direction of arrival estimation of quasi-stationary signals using unfolded coprime array," *IEEE Access*, vol. 5, pp. 6538–6545, 2017.
[16] H. Chen, H.-Z. Shao, and W.-Q. Wang, "Joint sparsity-based range-angle-dependent beampattern synthesis for frequency diverse array," *IEEE Access*, vol. 5, pp. 15152–15161, 2017.
[17] C. Mai, S. Lu, J. Sun, and G. Wang, "Beampattern optimization for frequency diverse array with sparse frequency waveforms," *IEEE Access*, vol. 5, pp. 17914–17926, 2017.
[18] R. Merino-Martínez *et al.*, "A review of acoustic imaging methods using phased microphone arrays," *CEAS Aeronaut. J.*, vol. 10, no. 1, pp. 197–230, Mar. 2019.

[19] W. Pannert and C. Maier, "Rotating beamforming-motion-compensation in the frequency domain and application of high-resolution beamforming algorithms," *J. Sound Vib.*, vol. 333, no. 7, pp. 1899–1912, Mar. 2014.
[20] M. Debrouwere and D. Angland, "Airy pattern approximation of a phased microphone array response to a rotating point source," *J. Acoust. Soc. Amer.*, vol. 141, no. 2, pp. 1009–1018, Feb. 2017.
[21] T. Zhou, Y. Sun, X. Zhang, W. Chen, and X. Huang, "Measurement of trailing edge noise from a heaving airfoil," in *Proc. 26th Int. Congress Sound Vib.*, 2019, pp. 1–8.
[22] W. Chen, B. Peng, R. P. Liem, and X. Huang, "Experimental study of airfoil-rotor interaction noise by wavelet beamforming," *J. Acoust. Soc. Amer.*, vol. 147, no. 5, pp. 3248–3259, 2020.
[23] W. Chen and X. Huang, "Wavelet-based beamforming for high-speed rotating acoustic source," *IEEE Access*, vol. 6, pp. 10231–10239, Jan. 2018.
[24] H. H. Murray, W. J. Devenport, W. N. Alexander, S. A. L. Glegg, and D. Wisda, "Aeroacoustics of a rotor ingesting a planar boundary layer at high thrust," *J. Fluid Mech.*, vol. 850, pp. 212–245, Sep. 2018.
[25] H. H. Murray, "Turbulence and sound generated by a rotor operating near a wall," M.S. thesis, Virginia Polytech. Inst. State Univ., Blacksburg, VI, USA, 2016.
[26] R. M. Martin and J. C. Hardin, "Spectral characteristics of rotor blade/vortex interaction noise," *J. Aircr.*, vol. 25, no. 1, pp. 62–68, Jan. 1988.
[27] B. Davoudi, S. Morris, and J. F. Foss, "Self-noise and wake velocity of an axial fan for different operating conditions," *AIAA J.*, vol. 54, no. 12, pp. 3918–3927, Dec. 2016.
[28] M.-J. Park and D.-J. Lee, "Sources of broadband noise of an automotive cooling fan," *Appl. Acoust.*, vol. 118, pp. 66–75, Mar. 2017.
[29] C. A. Kissner and S. Guérin, "Influence of wake and background turbulence on predicted fan broadband noise," *AIAA J.*, vol. 58, no. 2, pp. 659–672, Feb. 2020.
[30] I. Mezić, "Analysis of fluid flows via spectral properties of the koopman operator," *Annu. Rev. Fluid Mech.*, vol. 45, no. 1, pp. 357–378, Jan. 2013.
[31] G. Berkooz, P. Holmes, and J. L. Lumley, "The proper orthogonal decomposition in the analysis of turbulent flows," *Annu. Rev. Fluid Mech.*, vol. 25, no. 1, pp. 539–575, Jan. 1993.
[32] A. Towne, O. T. Schmidt, and T. Colonius, "Spectral proper orthogonal decomposition and its relationship to dynamic mode decomposition and resolvent analysis," *J. Fluid Mech.*, vol. 847, pp. 821–867, May 2018.
[33] M. O. Iqbal and F. O. Thomas, "Coherent structure in a turbulent jet via a vector implementation of the proper orthogonal decomposition," *J. Fluid Mech.*, vol. 571, pp. 281–326, Jan. 2007.
[34] B. R. Noack, W. Stankiewicz, M. Morzyński, and P. J. Schmid, "Recursive dynamic mode decomposition of transient and post-transient wake flows," *J. Fluid Mech.*, vol. 809, pp. 843–872, Nov. 2016.
[35] O. T. Schmidt and P. J. Schmid, "A conditional space-time POD formalism for intermittent and rare events: Example of acoustic bursts in turbulent jets," *J. Fluid Mech.*, vol. 867, Apr. 2019.
[36] J. Östh, B. R. Noack, S. Krajnović, D. Barros, and J. Borée, "On the need for a nonlinear subscale turbulence term in POD models as exemplified for a high-Reynolds-number flow over an ahmed body," *J. Fluid Mech.*, vol. 747, pp. 518–544, Apr. 2014.
[37] R. E. A. Arndt, D. F. Long, and M. N. Glauser, "The proper orthogonal decomposition of pressure fluctuations surrounding a turbulent jet," *J. Fluid Mech.*, vol. 340, pp. 1–33, Jun. 1997.
[38] K. E. Meyer, J. M. Pedersen, and O. Özcan, "A turbulent jet in crossflow analysed with proper orthogonal decomposition," *J. Fluid Mech.*, vol. 583, pp. 199–227, Jul. 2007.
[39] H. Bu, W. Yu, P.-W. Kwan, and X. Huang, "Wind-tunnel investigation on the compressive-sensing technique for aeroengine fan noise detection," *AIAA J.*, vol. 56, no. 9, pp. 3536–3546, Sep. 2018.
[40] W. Yu, Z. Ma, A. S. H. Lau, and X. Huang, "Analysis and experiment of the compressive sensing approach for duct mode detection," *AIAA J.*, vol. 56, no. 2, pp. 648–657, Feb. 2018.
[41] W. Yu, X. Wang, and X. Huang, "Dynamic modelling of heat transfer in thermal-acoustic fatigue tests," *Aerosp. Sci. Technol.*, vol. 71, pp. 675–684, Dec. 2017.
[42] W. Yu and X. Huang, "Compressive sensing based spinning mode detections by in-duct microphone arrays," *Meas. Sci. Technol.*, vol. 27, no. 5, Apr. 2016, Art. no. 055901.
[43] W. Yu and X. Huang, "Reconstruction of Aircraft engine noise source using beamforming and compressive sensing," *IEEE Access*, vol. 6, pp. 11716–11726, Aug. 2018.

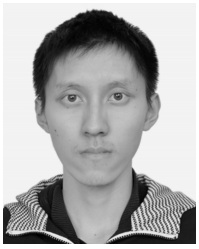

SICONG LIANG was born in Guilin, China, in 1997. He received the B.Eng. degree from Peking University, Beijing, China, in 2020, where he is currently pursuing the Ph.D. degree in aerospace engineering. His research interests include duct mode detection and deep learning's application in aerospace.

WANGQIAO CHEN was born in Mudanjiang, China, in 1994. He received the B.Eng. degree from Peking University, Beijing, China, in 2016, where he is currently pursuing the Ph.D. degree in aerospace engineering. He was a Research Assistant with The Hong Kong University of Science and Technology, from 2016 to 2017. His research interests include array signal processing and flow visualization for various aerospace applications.

RHEA P. LIEM received the Bachelor of Engineering degree from the School of Mechanical and Production Engineering, Nanyang Technological University, Singapore, the Master of Science (SM) degrees in computation for design and optimization and aeronautics/astronautics from the Massachusetts Institute of Technology (MIT), and the Ph.D. degree from the Multidisciplinary Design Optimization (MDO) Laboratory, University of Toronto Institute for Aerospace Studies (UTIAS), as a Vanier Canada Graduate Scholar. She is currently an Assistant Professor with the Department of Mechanical and Aerospace Engineering, The Hong Kong University of Science and Technology (HKUST). Her bachelor's study was supported by the Association of Southeast Asian Nations (ASEAN) with a four year merit-based Full Scholarship and the Master of Science degree was supported by the Singapore-MIT Alliance Fellowship Award. Her research interests include modeling and simulation of complex systems, in aircraft design and air transportation applications, and algorithmic development and applications of surrogate modeling techniques. She is an Amelia Earhart Fellow, in 2012.

XUN HUANG (Member, IEEE) was born in Hangzhou, China, in 1977. He received the B.Eng. degree in aerospace engineering from Northwestern Polytechnical University, Xi'an, China, in 1999, the M.Eng. degree in automatic control from Tsinghua University, Beijing, China, in 2002, and the Ph.D. degree in aeronautics and astronautics from the University of Southampton, Southampton, U.K., in 2006. He was a Research Engineer with the Shanghai Control Laboratory, GE Global Research Center, in 2003. He was a Research Assistant, in 2006, and a Research Fellow, in 2007. He was also a Lecturer with the School of Engineering Sciences, University of Southampton, in 2008. In 2009, he was an Associate Professor and a Professor with the College of Engineering, Peking University. Since 2015, he has been visiting the University of Cambridge and The Hong Kong University of Science and Technology and initiating research collaboration. He has authored over 80 refereed journal articles. He holds two patents. His research interests include control, acoustics, and array signal processing, especially for aerospace applications. He was a recipient of the Edison Technology Excellence Award, in 2003, the Award of Excellent Young Scholar from the National Science Foundation of China, in 2013, and the Newton Advanced Fellowship from the Royal Society, U.K., in 2015. He serves as an Editorial Board Member for the *International Journal of Aeroacoustics* and *Journal of Acta Mechanica Sinica*. He also serves as an Associate Editor for *Journal of the Acoustical Society of America*.